

# Optically Induced Interaction of Magnetic Moments in Hybrid Metamaterials

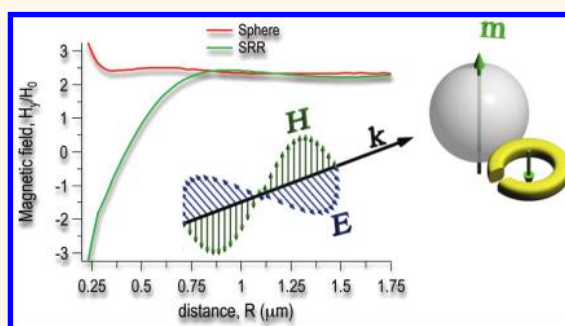
Andrey E. Miroshnichenko,<sup>†,\*</sup> Boris Luk'yanchuk,<sup>‡</sup> Stefan A. Maier,<sup>§</sup> and Yuri S. Kivshar<sup>†</sup>

<sup>†</sup>Nonlinear Physics Centre and Centre for Ultra-high Bandwidth Devices for Optical Systems (CUDOS), Research School of Physics and Engineering, Australian National University, Canberra ACT 0200, Australia, <sup>‡</sup>Data Storage Institute, Agency for Science, Technology and Research, 117 608 Singapore, and <sup>§</sup>Department of Physics, Imperial College London, London SW7 2AZ, U.K.

Metamaterials offer many novel possibilities to manipulate and control the propagation of electromagnetic waves.<sup>1,2</sup> Typical metamaterials are created by a system of resonant subwavelength elements for which electric and magnetic responses can be varied and modified independently. The artificial magnetism at high frequencies is based on the inductive response of normal metals,<sup>3</sup> and it was demonstrated for metal–dielectric “fishnet” structures<sup>3</sup> and arrays of split-ring resonators.<sup>4</sup> In such cases, the optically induced “ferromagnetic” (FM) ordering of induced magnetization of the whole structure is utilized in order to achieve the negative magnetic response required for left-handed metamaterials.<sup>5–9</sup> We would like to note that such terminology borrowed from solid-state physics should be used with caution. The difference between static and optically induced magnetization has been already discussed in the literature.<sup>10</sup> However, many novel magnetic phenomena are expected in systems with staggered magnetization, *i.e.*, with “antiferromagnetic” (AFM) ordering.<sup>11</sup> One of the well-known examples of such novel phenomena is related to the existence of giant magneto-resistance.<sup>12–14</sup>

A canonical subwavelength artificial magnetic “meta-atom” is represented by a familiar split-ring resonator (SRR) that consists of an inductive metallic ring with a gap. Such a SRR can support an eigenmode with a circular current that gives rise to a local magnetic dipole moment,<sup>15</sup> which can be considered as a magnetic counterpart for an electric dipole. This is one of the simplest examples demonstrating that a nonmagnetic material can possess a nonzero induced magnetization. By *nonmagnetic* material we mean a material whose bulk magnetization is zero

## ABSTRACT



We propose a novel type of hybrid metal–dielectric structures composed of silicon nanoparticles and split-ring resonators for advanced control of optically induced magnetic response. We reveal that a hybrid “metamolecule” may exhibit a strong distance-dependent magnetic interaction that may flip the magnetization orientation and support “antiferromagnetic” ordering in a hybrid metamaterial created by a periodic lattice of such metamolecules. The propagation of magnetization waves in the hybrid structures opens new ways for manipulating artificial “antiferromagnetic” ordering at high frequencies.

**KEYWORDS:** optical metamaterials · artificial magnetism · light-induced coupling

in the presence of a *static* magnetic field. The case of time-dependent fields becomes trickier since due to Maxwell's equations both electric and magnetic components intervene. There are other classical examples where the magnetization can be induced by electric field only,<sup>16</sup> including the inverse Faraday effect.<sup>17</sup> The latter allows creating static magnetization from rectified circular polarized light. The SRR-based design was the first and most frequently used for metamaterials, with unprecedented values of negative magnetic permeability at high frequencies.<sup>18,19</sup> However, the performance of SRR-based metamaterials at optical frequencies is limited by high conduction losses of the constitutive metallic elements and

\* Address correspondence to aem124@physics.anu.edu.au.

Received for review November 9, 2011 and accepted December 16, 2011.

Published online 10.1021/nn204348j

© XXXX American Chemical Society

the kinetic inductance of the electrons. Another example of plasmonic nanostructures that supports strong magnetic resonances is perforated semishells.<sup>20</sup> These structures can be viewed as 3D analogues of SRRs.

To improve the overall performance of metamaterials at optical frequencies, one can employ dielectric particles with low or negligible losses in the visible spectrum. By using the Mie theory<sup>21</sup> it can be analytically demonstrated that the scattering of electromagnetic waves by a small nonmagnetic dielectric particle may exhibit a strong magnetic resonance. This resonance occurs when the wavelength inside the particle  $\lambda_s = \lambda_0/n_s$  approximately equals its diameter  $2R_s$ , where  $\lambda_0$  is the incident wavelength and  $n_s$  and  $R_s$  are the refractive index and the radius of the particle, respectively. A nonzero magnetic dipole moment (coefficient  $b_1$  in Mie theory<sup>21</sup>) arises due to circulation of the displacement currents. The effect is similar to the appearance of the induced nonzero magnetization of SRRs, with the only difference that displacement currents do not contribute to Joule's heating. At such resonant conditions the tangential components of the electric field polarization are antiparallel on the different sides of the sphere along the propagation direction, resulting in a strong overlap with the magnetic mode. Thus, a dielectric particle can be considered as another example of a magnetic-dipole scatterer of an incident electromagnetic wave at the resonant wavelength. This yields an increased magnetic field in the near-field region around the particle. For the case of a silicon sphere with the radius in the range  $R = 40\text{--}100$  nm the magnetic resonance can be located in the visible spectrum.<sup>22</sup> This makes such particles the best candidates to achieve low-loss magnetic response at high frequencies. In the case of magnetic moments of different origin the overall magnetic response depends on the geometry of the system.

In this paper, we demonstrate that optically induced magnetic moments of a dielectric sphere and SRR can effectively interact with each other when they are placed in a close proximity (see Figure 1). An important finding of our study is the demonstration of the ability for staggered patterns to produce a distribution of the magnetic moments associated with optically induced AFM-like response. Although, these are dynamically excited states, at any given moment of time mutual magnetization of the neighboring elements is antiparallel, which allows us to call such a state AFM-like, in analogy with the spin ordering in solids. In addition, one- and two-dimensional lattices of such hybrid elements support novel types of magnetization waves. The AFM-like response of the hybrid metamaterials in the THz regime may offer a range of useful applications, including sensing of magnetic fields. We would like to stress that there is a principal difference between an optically induced magnetic dipole and a static magnet (compass needle). Namely, the static magnetic field does not influence the optically induced magnetic dipole. However, it can be used in the dynamic

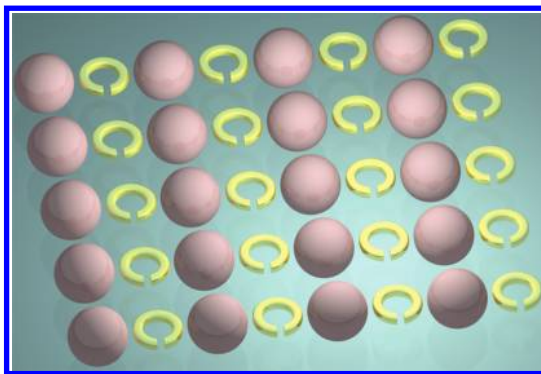


**Figure 1.** Schematic of a hybrid metal–dielectric structure consisting of silicon spheres coupled to copper split-ring resonators.

regime for optically induced magnetization, direct observation of a propagating spin waves,<sup>23</sup> and all-optical magnetic recording with the use of magneto-optical materials.<sup>24</sup> Also the effective generation of magnetization waves is similar to spin waves, which may carry electrical signals through a dielectric medium.<sup>25</sup>

## RESULTS AND DISCUSSION

We start our theoretical analysis by employing a coupled-dipole approach. In the long-wavelength limit, when the characteristic sizes of a dielectric sphere and SRR are much smaller than the wavelength of the incident light, namely,  $R_{s,SRR} \ll \lambda_0$ , their optical properties can be described by the effective dipoles

$$\mathbf{p}_1 = \varepsilon_0 \alpha_1 \mathbf{E}_0, \quad \mathbf{m}_{1,2} = \chi_{1,2} \mathbf{H}_0 \quad (1)$$

where  $\mathbf{p}_1$  and  $\mathbf{m}_1$  are the induced electric and magnetic dipoles of the dielectric sphere,  $\mathbf{m}_2$  is the magnetic dipole of the SRR,  $\alpha_s$ ,  $\chi_s$ , and  $\chi_{SRR}$  are the electric and magnetic polarizabilities, and  $\mathbf{E}_0$  and  $\mathbf{H}_0$  are the incident electric and magnetic fields. Since the electric response of the SRR is very weak, it can be neglected.

The effective polarizabilities of the sphere can be obtained from the corresponding scattering dipole coefficients  $a_1$  and  $b_1$  of the exact Mie solution<sup>21</sup>

$$\alpha_1 = 6\pi i \frac{a_1}{k^3}, \quad \chi_1 = 6\pi i \frac{b_1}{k^3} \quad (2)$$

where  $k = 2\pi/\lambda_0$  is a wavenumber and the magnetic polarizability of SRR can be approximated as<sup>15</sup>  $\chi_2 = F\omega^2/(\omega_0^2 - \omega^2)$ , where  $\omega_0$  is the resonant frequency of a single SRR and  $F$  is a geometric factor.

To study the optical response of an interacting dielectric sphere and a SRR, we employ the method of coupled electric and magnetic dipoles<sup>26–28</sup> and write the following system of equations:

$$\begin{aligned} \mathbf{p}_1 &= \alpha_1 \left\{ \varepsilon_0 \mathbf{E}_0 - \frac{d}{c} (\mathbf{n} \times \mathbf{m}_2) \right\}, \\ \mathbf{m}_1 &= \chi_1 \{ \mathbf{H}_0 + \mathbf{a} \mathbf{m}_2 + b (\mathbf{n} \cdot \mathbf{m}_2) \mathbf{n} \}, \\ \mathbf{m}_2 &= \chi_2 \{ \mathbf{H}_0 + \mathbf{a} \mathbf{m}_1 + b (\mathbf{n} \cdot \mathbf{m}_1) \mathbf{n} - dc (\mathbf{n} \times \mathbf{p}_1) \} \end{aligned} \quad (3)$$

where  $c = 1/(\epsilon_0\mu_0)^{1/2}$  is the speed of light,  $\mathbf{n}$  is a unit vector pointing from the sphere to the SRR, and the coefficients  $a$ ,  $b$ , and  $d$  describe the interaction between dipoles.<sup>29</sup>

$$\begin{aligned} a &= \frac{e^{ikR}}{4\pi R} \left( k^2 - \frac{1}{R^2} + \frac{ik}{R} \right), \\ b &= \frac{e^{ikR}}{4\pi R} \left( -k^2 + \frac{3}{R^2} - \frac{3ik}{R} \right), \\ d &= \frac{e^{ikR}}{4\pi R} \left( k^2 + \frac{ik}{R} \right) \end{aligned} \quad (4)$$

where  $R$  is the distance between the sphere and SRR.

For a sphere and SRR being aligned along the  $x$ -axis [ $\mathbf{n} = (1,0,0)$ ] and the incident light propagating along the  $z$ -direction [ $\mathbf{k} = (0,0,k)$ ], polarized with the magnetic field along the  $y$ -axis [ $\mathbf{H}_0 = (0,H_y,0)$ ], the solution can be written as follows:

$$\begin{aligned} m_{1,y} &= \frac{(1 + a\chi_2 + d^2\alpha_1\chi_2)}{(1 - a^2\chi_1\chi_2 + d^2\alpha_1\chi_2)}\chi_2H_y, \\ m_{2,y} &= \frac{(1 + a\chi_1)}{(1 - a^2\chi_1\chi_2 + d^2\alpha_1\chi_2)}\chi_2H_y, \\ p_{1,x} &= \epsilon_0\alpha_1E_x, p_{1,z} = -\left(\frac{d}{c}\right)\alpha_1m_{1,y} \end{aligned}$$

with all other components vanishing. This simple solution gives us a useful insight, and it provides the information about the optical response of the hybrid system in different limiting cases. For the case of a far separated sphere and SRR, their magnetization will be identical to the uncoupled system since  $a, d \rightarrow 0$  with  $R \rightarrow \infty$ , resulting in  $m_{(1,2),y} = \chi_{1,2}H_y$ . However, in the opposite limit when the sphere and SRR are placed very close to each other ( $R \rightarrow 0$ ), the situation changes dramatically. The electric dipole moment of the sphere contributes strongly to the magnetization of the sphere itself since the cross-coupling coefficient  $d^2 \propto R^{-4}$  becomes larger in the leading order compared to the self-coefficient  $a \propto R^{-3}$  for very small distances  $R \rightarrow 0$ . This self-action of the longitudinal electric dipole on the sphere magnetization may result in the opposite magnetic response compared to the case of the uncoupled pair, depending on the relative signs of  $\alpha_1$  and  $\chi_2$ . Thus, by placing a sphere and SRR in close proximity, we may expect the appearance of an *AFM-like response* of the whole structure.

On the basis of the general analysis presented above, we consider a small silicon sphere interacting with a set of identical copper SRRs. To enhance the magnetic response of the SRR, we use a multistack with five layers. We optimize the parameters to ensure strong interaction between these two elements. In particular, the decoupled dielectric sphere and SRR have close magnetic resonances  $\omega_s = 281$  THz and  $\omega_{\text{SRR}} = 250$  THz, respectively (see Figure 2a). In our numerical simulations, we confirm directly the existence of a strong optically induced magnetic coupling in the hybrid metamolecule. We observe that,

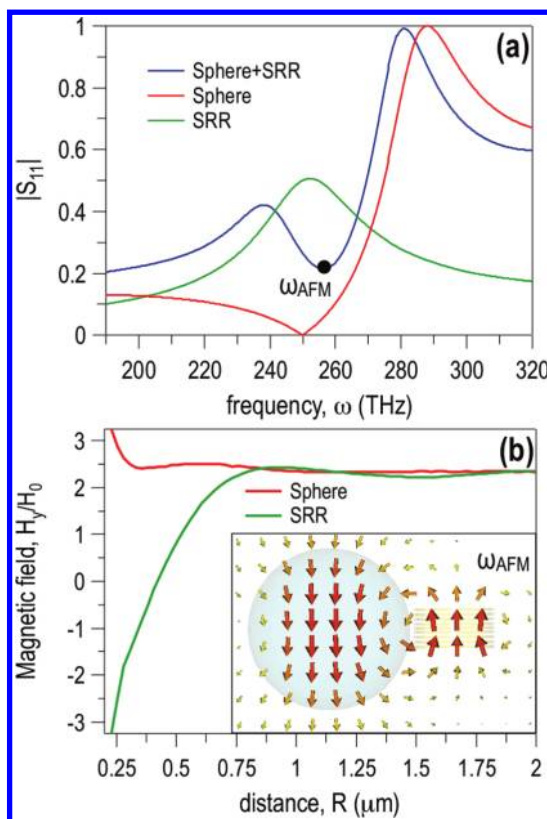


**Figure 2.** Magnetic response of a silicon sphere coupled to a multistack of SRRs. (a) Reflection curves of single elements (single silicon sphere and multistack of SRRs) and of the coupled structure. Two peaks of the coupled system correspond to the magnetic resonances of isolated elements. Resonant dip corresponds to the AFM-like excitation with staggered magnetic polarizabilities. (b) Dependence of the induced magnetization of the sphere and SRRs on the distance between at the resonant frequency  $\omega_{\text{AFM}} = 257$  THz. Below the critical distance  $R_{\text{cr}} \approx 1 \mu\text{m}$  the ferromagnetic-like magnetization switches to antiferromagnetic. Inset shows the distribution of the induced magnetic field at the AFM-like resonance.

in addition to red-shifting independent magnetic resonances of the sphere and SRRs where the magnetic response is dominated by one or another component, there appears a novel, *AFM-like response* with antiparallel magnetization of both the elements of comparable strength in the vicinity of the SRR's magnetic resonance  $\omega_{\text{AFM}} = 257$  THz. The longitudinal electric dipole moment of the sphere induced by SRRs plays an important role in the flipping the sign of magnetization, when two elements are placed in close proximity. Indeed, by studying the dependence of the magnetization on the distance between two elements, as summarized in Figure 2b, we clearly observe that both elements exhibit a FM-like response for larger distances  $R > R_{\text{cr}}$ , which changes to the AFM-like response for smaller distances  $R < R_{\text{cr}}$ , with staggered magnetization. The distance-dependent magnetic response is a unique feature of a hybrid structure. Such an effect does not exist in systems consisting of either silicon spheres<sup>22</sup> or SRRs<sup>30,31</sup> only, and it provides the opportunity

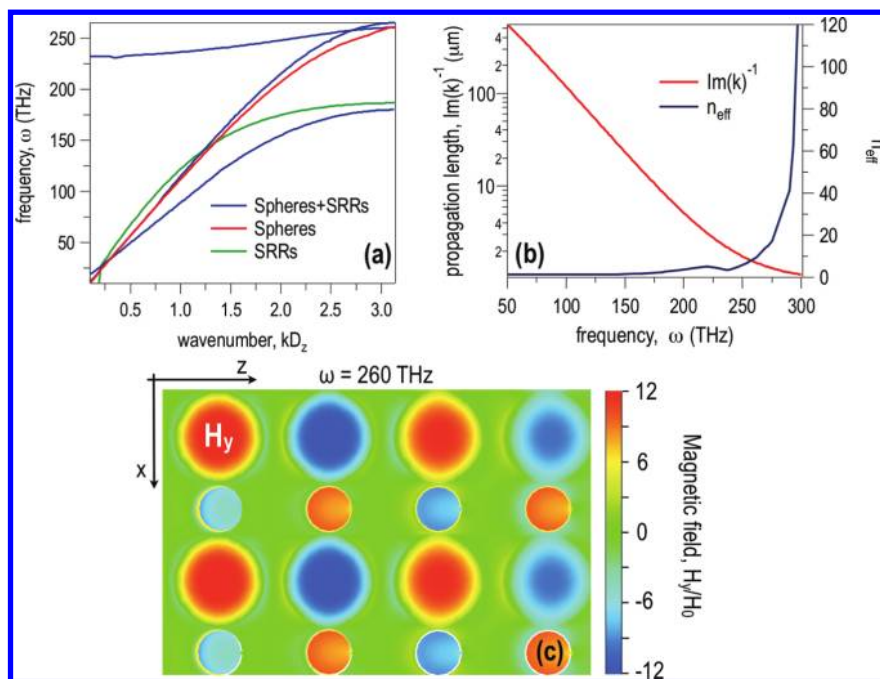


**Figure 3.** (a) Comparison of the dispersion diagrams of two-dimensional lattices of spheres, SRRs, and hybrid sphere–SRR system with the periodicity in the  $z$ -direction  $D_z = 350$  nm. (b) Calculated propagation length and effective refractive index of a finite structure. (c) Magnetic field distribution  $H_y$  of a two-dimensional structure at the resonant frequency  $\omega = 260$  THz. This gives a typical example of the staggered two-dimensional checkerboard magnetization of the hybrid structure.

to control the overall effective magnetic response. Thus, the role of SRRs in our hybrid metamaterial is to control the relative phase.

Next, we consider a two-dimensional lattice of the hybrid metamolecules that corresponds to a novel hybrid metamaterial. Such periodic lattices of spherical particles can be fabricated by laser-induced transfer technique.<sup>32</sup> Due to spherical symmetry the induced magnetic dipole of the spheres is always parallel to the exciting magnetic field component. Thus, we consider an in-plane TM polarized wave at normal incidence. The AFM-like response of a single element implies that the periodic structure may also exhibit a staggered magnetization in the transverse direction, which is of a resonant origin, and it is closely related to the AFM-like response. However, in periodic structures we concentrate on staggered magnetization in the longitudinal direction along the propagation. In Figure 3a we plot the dispersion diagram of a two-dimensional lattice of coupled hybrid metamolecules with a period  $D_z = 350$  nm in the  $z$ -direction and compare it with the dispersions of the corresponding “monatomic” lattices of silicon spheres and SRRs, with the same period. We observe clearly the appearance of a new branch in the coupled system corresponding to the staggered AFM-like magnetization in the transverse direction. It is interesting that in the vicinity of the band edge one can see a staggered magnetic response in the longitudinal direction too, *i.e.*, a checkerboard pattern of the total two-dimensional magnetization. There could be several reasons for that, including (i) a staggered

induced magnetic field along the propagation at the band edge and (ii) interaction of induced longitudinal electric dipoles of dielectric spheres. Both of these conditions are met for the AFM branch near the frequency  $\omega = 260$  THz, which corresponds to the AFM-like resonance of a single metamolecule (see Figure 2a) and the band edge of the two-dimensional structure (see Figure 3a). The numerical results for the excitation at this particular frequency are shown in Figure 3c. Moreover, this frequency corresponds to the crossing of two dispersion curves, where mostly dielectric spheres are excited, leading to strong localization of the AFM-like response in a low-loss dielectric material. It also results in a stronger magnetic interaction between spheres and SRRs, where the resonantly excited longitudinal dielectric dipoles of the spheres play an essential role in magnetization along the propagation. In this way, the control of the mutual phase of magnetization becomes possible. We find that a robust staggered magnetization pattern of dielectric spheres in the vicinity of the AFM-like resonance of a single hybrid element depends weakly on the periodicity in the  $z$ -direction up to the values of  $D_z = 600$  nm (see Figure 2a). For larger periods, the dispersion diagram of the coupled systems changes significantly, and the AFM branch shifts away from the resonant frequency.

To estimate the propagation length of the induced magnetization waves in such a structure, we employ the method recently suggested in ref 33. This method allows us to extract complex propagation constants of

the Bloch modes based on a finite number of sample points per period. The results are summarized in Figure 3c, where the propagation length is inversely proportional to the imaginary part of the corresponding wavevector,  $\sim \text{Im}(k)^{-1}$ . It decays exponentially with frequency, and the AFM-like resonance  $\omega_{\text{AFM}} = 257$  THz corresponds to six periods of the structure. At the same time, the effective refractive index, calculated as a ratio between the real part of the wavevector and its free space counterpart  $n_{\text{eff}} = \text{Re}(k_{\text{hybrid}})/k$ , becomes relatively large;  $n_{\text{eff}} \approx 10$ . It corresponds to the regime with a slow phase velocity.

## CONCLUSION

We have studied the optically induced interaction of magnetic moments of hybrid metal–dielectric structures consisting of dielectric spheres and split-ring resonators. We have revealed that each element of such a hybrid structure exhibits a strong magnetic response in the THz frequency range, and coupling of

two different elements leads to a strong interaction of magnetic moments between the spheres and split-ring resonators. On the basis of the coupled-dipole model, we have demonstrated an important role of resonantly induced longitudinal electric dipoles in the formation of an AFM-like response with a staggered magnetization below a critical separation. Arranging the hybrid meta-atoms into a two-dimensional lattice allows creating a hybrid metamaterial supporting staggered magnetization in the longitudinal direction due to the magnetic interaction between the dielectric spheres. A weak dependence of the staggered magnetization of the dielectric spheres on the distance between them at the AFM-like resonance of a single metamolecule indicates a significant contribution of the induced longitudinal electric dipoles into the overall magnetic interaction. We believe this approach opens novel possibilities for the manipulation and control of artificial “antiferromagnetism” at optical frequencies.

## METHODS

**Mie Theory.** The optical properties of a single dielectric sphere can be analyzed in the framework of the Mie theory.<sup>21</sup> It provides full analytical insight into the problem of the light scattering by a sphere. By using this method, the frequencies of the electric and magnetic resonances are calculated. In contrast to plasmonic particles, where the electromagnetic field is negligible inside the particle and all resonances can be estimated by using the Mie scattering coefficients only, the situation is completely different for dielectric particles. In the latter case, the electromagnetic field is nonzero inside the particle, and the accurate position of the resonances should be calculated based on the internal field enhancement for a particular mode. Our analysis reveals that magnetic resonance takes place when the wavelength inside the particle roughly equals the particle's diameter.

**Method of Coupled Electric and Magnetic Dipoles.** We employ the method of coupled electric and magnetic dipoles to estimate the excitation states of the hybrid system consisting of a dielectric sphere and SRR.<sup>26</sup> The electric and magnetic polarizabilities of the sphere can be obtained from the corresponding Mie scattering coefficients. Although we are dealing with the dielectric nonmagnetic sphere, it may support resonantly excited magnetic modes with nonzero magnetization, which will scatter light similarly to a magnetic dipole in the far field. Thus, in addition to electric polarizability, it allows us to assign an effective magnetic polarizability to the dielectric sphere as well. Under the considered excitation conditions, the electronic response of the SRR can be neglected.

**Numerical Simulations.** All numerical results are obtained using CST Microwave Studio. In our simulations, we take a Si sphere with radius  $R = 150$  nm and permittivity  $\epsilon = 12.25$ . For SRR we consider copper with an inner radius  $R_1 = 70$  nm, outer radius  $R_2 = 75$  nm, thickness  $h = 5$  nm, and gap width  $g = 10$  nm. The choice of the material might not be optimal, and for practical realization it is better to use some alloys of weakly dissipating plasmonic materials, as was recently indicated in ref 34.

The dispersion relations, the effective propagation length, and the refractive index were retrieved by using the Bloch-mode extraction method from near-field data in periodic arrays.<sup>33</sup>

**Acknowledgment.** The authors thank M. Decker, B. Ivanov, A. Slavin, H. Giessen, and M. I. Dyakonov for useful discussions.

The work was supported by the Australian Research Council through Discovery, Future and Federation Fellowships, as well as Centre of Excellence CUDOS in Australia and the Leverhulme Trust in the UK. The research presented in this paper is supported by the Agency for Science, Technology and Research (A\*STAR): SERC Metamaterials Program on Superlens, grant no. 092 154 0099 and A\*STAR TSRP Program, grant no. 102 152 0018.

## REFERENCES AND NOTES

1. *Electromagnetic Metamaterials: Physics and Engineering Explorations*; Engheta, N.; Ziolkowski, R. W., Eds.; Wiley-IEEE Press: New York, 2006.
2. *Metamaterials: Theory, Design, and Applications*; Cui, T. J.; Smith, D.; Liu, R., Eds.; Springer-Verlag: Heidelberg, 2009.
3. Shalaev, V. M. Optical Negative Index Metamaterials. *Nat. Photon* **2007**, *1*, 41–48.
4. Lahiri, B.; McMeekin, S. G.; Khokhar, A. Z.; De la Rue, R. M.; Johnson, N. P. Magnetic Response of Split Ring Resonators (SRRs) at Visible Frequencies. *Opt. Express* **2010**, *18*, 3210–3218.
5. Liu, H.; Genov, D. A.; Wu, D. M.; Liu, Y. M.; Steele, J. M.; Sun, C.; Zhu, S. N.; Zhang, X. Magnetic Plasmon Propagation Along a Chain of Connected Subwavelength Resonators at Infrared Frequencies. *Phys. Rev. Lett.* **2006**, *97*, 243902.
6. Wang, S. M.; Li, T.; Liu, H.; Wang, F. M.; Zhu, S. N.; Zhang, X. Magnetic Plasmon Modes in Periodic Chains of Nanosandwiches. *Opt. Express* **2008**, *16*, 3560–3565.
7. Liu, N.; Fu, L.; Kaiser, S.; Schweizer, H.; Giessen, H. Plasmonic Building Blocks for Magnetic Molecules in Three-Dimensional Optical Metamaterials. *Adv. Mater.* **2008**, *20*, 3859–3865.
8. Liu, N.; Giessen, H. Three-Dimensional Optical Metamaterials As Model Systems for Longitudinal and Transverse Magnetic Coupling. *Opt. Express* **2008**, *16*, 21233–21238.
9. Ghadarghad, S.; Mosallaei, H. Coupled Dielectric Nanoparticles Manipulating Metamaterials Optical Characteristics. *IEEE Trans. Nanotechnology* **2009**, *8*, 582–594.
10. Liu, N.; Giessen, H. Coupling Effects in Optical Metamaterials. *Angew. Chem.* **2010**, *49*, 9838–9852.
11. Liu, N.; Mukherjee, S.; Bao, K.; Brown, L. V.; Dorfmueller, J.; Nordlander, P.; Halas, N. J. Magnetic Plasmon Formation and Propagation in Artificial Aromatic Molecules. *Nano Lett.* **2011**, accepted.

12. Grünberg, P.; Schreiber, R.; Pang, Y.; Brodsky, M. B.; Sowers, H. Layered Magnetic Structures: Evidence for Antiferromagnetic Coupling of Fe Layers across Cr Interlayers. *Phys. Rev. Lett.* **1986**, *57*, 2442–2445.
13. Baibich, M. N.; Broto, J. M.; Fert, A.; Nguyen an Dau, F.; Petroff, F.; Etienne, P.; Creuzet, G.; Friederich, A.; Chazelas, J. Giant Magnetoresistance of (001)Fe/(001)Cr Magnetic Superlattices. *Phys. Rev. Lett.* **1988**, *61*, 2472–2475.
14. Fullerton E. E.; Schuller I. K. The 2007 Nobel Prize in Physics: Magnetism and Transport at the Nanoscale. *ACS Nano* **2007**, *1*, 384–389.
15. Pendry, J. B.; Holden, A. J.; Robbins, D. J.; Stewart, W. J. Magnetism from Conductors, and Enhanced Non-Linear Phenomena. *IEEE Trans. Microwave Theory Tech.* **1999**, *47*, 2075–2084.
16. Tamm, I. E. *Basics of Theory of Electricity* [in Russian]; FizMatLit: Moscow, 2003; pp 539–543.
17. Stanciu, C. D.; Hansteen, F.; Kimel, A. V.; Kirilyuk, A.; Tsukamoto, A.; Itoh, A.; Rasing, Th. All-Optical Magnetic Recording with Circularly Polarized Light. *Phys. Rev. Lett.* **2007**, *99*, 047601.
18. Soukoulis, C. M.; Linden, S.; Wegener, M. Negative Refractive Index at Optical Wavelengths. *Science* **2007**, *315*, 47–49.
19. Soukoulis, C. M.; Wegener, M. Past Achievements and Future Challenges in the Development of Three-Dimensional Photonic Metamaterials. *Nat. Photon.* **2011**, *5*, 523–530.
20. Mirin, N. A.; Ali, T. A.; Nordlander, P.; Halas, N. J. Perforated Semishells: Far-Field Directional Control and Optical Frequency Magnetic Response. *ACS Nano* **2010**, *4*, 2701–2712.
21. Bohren, C. F.; Huffman, D. R. *Absorption and Scattering of Light by Small Particles*; Wiley: New York, 1998; pp 111–117.
22. Evlyukhin, A. B.; Reinhardt, C.; Seidel, A.; Luk'yanchuk, B.; Chichkov, B. N. Optical Response Features of Si Nanoparticle Arrays. *Phys. Rev. B* **2010**, *82*, 045404.
23. Madami, M.; Bonetti, S.; Consolo, G.; Tacchi, S.; Carlotti, G.; Gubbiotti, G.; Mancoff, F. B.; Yar, M. A.; Ekerman, J. Direct Observation of a Propagating Spin Wave Induced by Spin-Transfer Torque. *Nat. Nanotechnol.* **2011**, *6*, 635–638.
24. Temnov, V. V.; Armelles, G.; Woggon, U.; Guzatov, D.; Cebollada, A.; Garcia-Martin, A.; Garcia-Martin, J.-M.; Thomay, T.; Leitenstorfer, A.; Bratschitsch, R. Active Magneto-Plasmonics in Hybrid Metal-Ferromagnet Structures. *Nat. Photon* **2010**, *4*, 107–111.
25. Kajiwara, Y.; Harii, K.; Takahashi, S.; Ohe, J.; Uchida, K.; Mizuguchi, M.; Umezawa, H.; Kawai, H.; Ando, K.; Takanashi, K.; *et al.* Transmission of Electrical Signals by Spin-Wave Interconversion in a Magnetic Insulator. *Nature* **2010**, *464*, 262–266.
26. Mulholland, G. W.; Bohren, C. F.; Fuller, K. A. Light Scattering by Agglomerates: Coupled Electric and Magnetic Dipole Method. *Langmuir* **1994**, *10*, 2533–2546.
27. Garcá-Camara, B.; Moreno, F.; Gonzalez, F.; Martin, O. J. F. Light Scattering by an Array of Electric and Magnetic Nanoparticles. *Opt. Express* **2010**, *18*, 10001–10015.
28. Chaumeta, P. C.; Rahmani, A. Coupled-Dipole Method for Magnetic and Negative-Refractive Materials. *J. Quant. Spectrosc. Radiat. Transfer* **2009**, *110*, 22–29.
29. Jackson, J. D. *Classical Electrodynamics*; Wiley: New York, 1975; pp 407–416.
30. Decker, M.; Linden, S.; Wegener, M. Coupling Effects in Low-Symmetry Planar Split-Ring Resonator Arrays. *Opt. Lett.* **2009**, *34*, 1579–1581.
31. Decker, M.; Burger, S.; Linden, S.; Wegener, M. Magnetization Waves in Split-Ring-Resonator Arrays: Evidence for Retardation Effects. *Phys. Rev. B* **2009**, *80*, 193102.
32. Kuznetsov, A. I.; Evlyukhin, A. B.; Goncalves, M. R.; Reinhardt, C.; Koroleva, A.; Arnedillo, M. L.; Kiyani, R.; Marti, O.; Chichkov, B. N. Laser Fabrication of Large-Scale Nanoparticle Arrays for Sensing Applications. *ACS Nano* **2011**, *5*, 4843–4849.
33. Ha, S.; Sukhorukov, A. A.; Dossou, K. B.; Botten, L. C.; de Sterke, C. M.; Kivshar, Yu. S. Bloch-Mode Extraction from Near-Field Data in Periodic Waveguides. *Opt. Lett.* **2009**, *34*, 3776–3778.
34. Boltasseva, A.; Atwater, H. A. Low-Loss Plasmonic Metamaterials. *Science* **2011**, *331*, 290–291.